Advanced Ceramics Progress: Vol. 8, No. 2, (Spring 2022) 53-60

Materials and Energy Research Center
MERC

Contents lists available at ACERP

Advanced Ceramics Progress

Journal Homepage: www.acerp.ir

Original Research Article

A Comparative Study on the Phase Stability of ZrO_2-8 wt. % Y_2O_3 : Nano- and Micro-Particles

Milad Bahamirian [a, *]

[a] *Assistant professor, Department of Mining and Metallurgical Engineering, Yazd University, Yazd, Yazd, Iran*

* Corresponding Author Email: m.bahamirian@yazd.ac.ir (M. Bahamirian)

URL: https://www.acerp.ir/article_159835.html

ARTICLE INFO

Article History:

Received 17 July 2022
Received in revised form 05 September 2022
Accepted 24 September 2022

Keywords:

Thermal Barrier Coatings (TBCs)
YSZ : ZrO_2-8 wt. % Y_2O_3
Wet-Chemical Method
Phase Stability

ABSTRACT

At temperatures above 1200 °C, the phase instability of micro-YSZ : ZrO_2-8 wt. % Y_2O_3 is one of the major causes of damage to Thermal Barrier Coatings (TBCs) of the latest generation of gas turbines. In this study, nano-YSZ was produced using a wet chemical method to improve the phase stability of micro-YSZ. The phase stability of both synthesized nano-YSZ and commercially available micro-YSZ was examined after 50 h of heat treatment at 1300 °C. The data obtained from X-Ray Diffraction (XRD) analysis of nano-YSZ confirmed the formation of the non-transformable tetragonal (tetragonality parameter : $\frac{c}{a\sqrt{2}} < 1.01$) phase of ZrO_2 and its improved stability followed by heat treatment. Micro-YSZ, however, was decomposed into two new phases, i.e., monoclinic and cubic ZrO_2 with the wight percentages of 38 % and 62 wt. %, respectively, under comparable conditions. The morphological features of nano-YSZ were assessed by Field Emission Scanning Electron Microscopy (FESEM), the results of which confirmed the formation of YSZ nanoparticles with an average size of 40 nm. According to the findings, nano-YSZ could be a suitable candidate for use in TBCs of the next generations of gas turbines.

https://doi.org/10.30501/acp.2022.352174.1097

1. INTRODUCTION

Thermal Barrier Coatings (TBCs) have numerous applications in the hot areas of gas turbines and aviation engines that protect metallic components from the damaging effects of combustion chamber heat [1-3]. TBCs are typically deposited on hot pieces (with Ni and Co-based superalloys) by thermal spray techniques. They include two layers: (i) a bond coat of metallic elements with the composition MCrAlY (M could be Ni or Co) that provides proper resistance to high-temperature oxidation [4-6] and hot corrosion [7-9] and (ii) a ceramic top coat [2,3]. For this reason, coat compositions have been developed based on ZrO_2 that are characterized by excellent properties such as low proper thermal conductivity ($k_{top\ coat}$ = 0.7-2.4 W/mK), thermal expansion coefficient ($\alpha_{top\ coat}$ ~ 7.5-10.5×10^{-6} K^{-1}) that is relatively compatible with the substrate ($\alpha_{superalloy}$ ~ 15-17×10^{-6} K^{-1} and $\alpha_{bond\ coat}$ ~ 10-12×10^{-6} K^{-1}), and resistance to high-temperature oxidation and hot corrosion as well as the thermal shock [2,3,10].

ZrO_2 can be found in three allotropic forms namely monoclinic (m), tetragonal (t), and cubic (c). The phase transformation from m-ZrO_2 to t-ZrO_2 is reversible that occurs at ~ 1170 °C while such transformation to m-ZrO_2 phase takes place at ~ 950 °C during the cool-down cycle.

Please cite this article as: Bahamirian M., "A Comparative Study on the Phase Stability of ZrO_2-8 wt. % Y_2O_3 : Nano- and Micro-Particles", ***Advanced Ceramics Progress***, Vol. 8, No. 2, (2022), 53-60. https://doi.org/10.30501/acp.2022.352174.1097

This phase transition can result in a volume variation in the range of 3-5 %, thus leading to cracks formation and eventually disintegration [2,3,11,12]. Stabilizing oxides such as Y_2O_3, MgO, CaO, and CeO_2 are used to prevent transition in the cool-down cycles [10,13]. One of the most well-known and commonly used compositions in this area is Y_2O_3-stabilized ZrO_2 (ZrO_2-8 wt. % Y_2O_3 or YSZ) [3].

Incorporation of the stabilizers into ZrO_2 leads to the formation of the non-transformable tetragonal phase (t'). The t´-ZrO_2 phase is crystallographically similar to the t-ZrO_2 phase; however, it has a smaller tetragonality ($\frac{c}{a\sqrt{2}}$, "c" and "a" represent the lattice parameters of the tetragonal ZrO_2 system) than that of its counterpart. During the cool-down cycles, such a phase will not change into m-ZrO_2 [14]. This phase (t´-ZrO_2) also possesses lower thermal conductivity [15] and better mechanical properties [16] than those of the other ZrO_2 phases. Therefore, this phase is highly favorable in the TBCs [17-19].

According to Equation (1), two phases of Y-rich (c-ZrO_2) and Y-dilute (t-ZrO_2) will be formed in micro-YSZ at the temperatures above 1200 °C. A phase transition from
t'-ZrO_2 to t-ZrO_2 also occurs in the micro-YSZ at temperatures above 1200 °C after which, the t-ZrO_2 will be transformed into m-ZrO_2 by cooling down to the ambient temperature [12].

$$\begin{matrix} \text{T-prime} \xrightarrow{1200\,^{\circ}\text{C (Heating)}} \text{Tetragonal and} \\ \text{Cubic} \xrightarrow{950^{\circ}\text{C (Cooling)}} \text{Cubic + Monoclinic} \end{matrix} \quad (1)$$

Recent studies [4,7,12,20-23] have emphasized the role of smaller ZrO_2 particles in decreasing the tetragonality and enhancing the stability of the t´-ZrO_2 by using the nano-TBCs in the new generation of turbines that can operate at temperatures above 1200 °C. Given the increasing demands for such new generation of gas turbines, the development of ZrO_2-based TBCs requires more precise investigations.

Several methods for production of ceramic nanoparticles have been proposed to date including mechanical milling, chemical procedures, hydrothermal synthesis, chemical vapor synthesis, co-precipitation, and sol-gel techniques, to name a few [17,23,24]. Low synthesis temperature, cost-effectiveness, controlled synthesis parameters, and remarkable capacity to control the chemical composition are among the advantages of the co-precipitation process [23].

To the best of our knowledge, a limited number of studies have addressed these powders and their applications. Therefore, the necessity of investigating the high-temperature phase stability behavior of nano-YSZ powders comes to the fore. The present study used a co-precipitation approach for the synthesis of nano-YSZ. After 50 hours of heat treatment at 1300 °C, the phase stability of the samples was evaluated, and the results were compared with those of the commercial micro-YSZ.

2. MATERIALS AND METHODS

Co-precipitation process is required to prepare nano-YSZ powder. Figure 1 lists the steps required for the synthesis process.

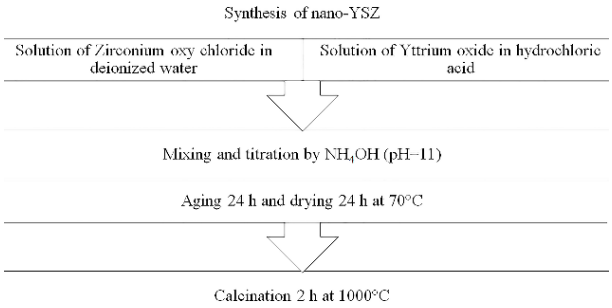

Figure 1. Procedure for the experimental synthesis of nano-YSZ through the co-precipitation method

$ZrOCl_2.8H_2O$ and Y_2O_3 with a purity of 99.9 % (Table 1) were used to supply Zr^{4+} and Y^{3+}, respectively.

TABLE 1. Chemical composition of materials used in fabricating nano-YSZ

Material	Chemical Formula	Purity	Company
Zirconium Oxychloride	$ZrOCl_2.8H_2O$	99.9 %	Merck
Yttrium Oxide	Y_2O_3	99.9 %	Merck

Y_2O_3 was dissolved in HCl to release Y^{3+} ions, as seen in Figure 1. Then, $ZrOCl_2.8H_2O$ was dissolved in double-distilled water. The solutions were mixed, and NH_4OH was gradually added to accelerate the reaction by keeping the pH above 11. The precipitate was rinsed with distilled water and passed through the appropriate filters. It was then dried for 24 hours at 70 °C. The precipitates were then calcined for two hours at 1000 °C.

To investigate the phase stability, micro-YSZ (Metco 204NS-G: ZrO_2-8 wt. % Y_2O_3) and nano-YSZ samples were heat-treated for 50 h at 1300 °C in five-hour cycles. The heating rate was measured as 10 °C/min at the temperatures ranging from the room temperature to 1300 °C and once the peak temperature is reached, the samples were kept for five hours and finally cooled down to the room temperature at the furnace cooling rate. This procedure was selected considering the parameters generally used for cyclic high temperature phase stability of TBCs [12,25]. The crystallographic variation of the samples was assessed at four intervals of t = 0, 10, 20, and 50 h.

To investigate the phases and morphological features

of micro-YSZ and nano-YSZ samples, Field Emission Scanning Electron Microscopy (FESEM) and X-Ray Diffraction (XRD) techniques were employed. Table 2 lists the characteristics of the applied techniques. Material Analysis Using Diffraction (MAUD) software was also for quantitative analysis of the XRD results through Rietveld refinement technique.

TABLE 2. Specifications and parameters of analysis equipment

Equipment	Equipment Model	Parameters
FESEM	MIRA3TESCAN-XMU	
XRD	Philips X'pert X-Ray Diffraction	2θ = 20 - 80° Step Size = 0.02 Time per Step = 0.5 s $\lambda_{Cu\ k\alpha}$ = 1.540598 Å 40 kV, 40 mA T = 25 °C

3. RESULTS AND DISCUSSION

Figure 2 depicts the results of XRD and FESEM analyses of commercial micro-YSZ powder before and after heat treatment (0, 10, 20, and 50 h) at 1300 ºC.

According to Figure 2, the commercial micro-YSZ powder contained a tetragonal ZrO_2 phase (JCDPS: # 01-082-1242). The micro-YSZ, however, exhibited some weak peaks of monoclinic ZrO_2 (JCDPS: # 01-078-1807) amounting to 7 wt. % according to the Rietveld method.

Figure 3 Shows the results of XRD and FESEM analysis for the synthesized nano-YSZ powder before (calcination at 1000 ºC for 2 h) and after heat-treatment (0, 10, 20, and 50 h) at 1300 ºC.

According to Figure 3, the nano-YSZ powder has a tetragonal ZrO_2 phase (JCDPS: # 01-082-1242). However, it exhibits some weak peaks of monoclinic ZrO_2 (JCDPS: # 01-078-1807) amounting to 3 wt. % according to the Rietveld refinement method.

Tetragonality ($\frac{c}{a\sqrt{2}}$), is a determining factor in investigating the stability of the tetragonal phase [23,26]. The tetragonality of the non-transformable (t') and transformable (t) tetragonal phases can be separated. If $\frac{c}{a\sqrt{2}} > 1.01$, the transformable tetragonal phase is stable. On the contrary, if $\frac{c}{a\sqrt{2}} < 1.01$, the non-transformable tetragonal phase is stable [23,27]. Since the calculated tetragonality values of the synthesized nano-YSZ and commercial micro-YSZ (by the Rietveld method) were $\frac{c}{a\sqrt{2}} = \frac{5.163}{3.645\sqrt{2}} = 1.001$ and $\frac{c}{a\sqrt{2}} = \frac{5.177}{3.641\sqrt{2}} = 1.005$, respectively, both samples had a non-transformable tetragonal phase of ZrO_2 before heat treatment at 1300 ºC.

According to Figure 2, the peaks related to 2θ = 27-33° (111) and 2θ = 72-76° (400) (corresponding to the monoclinic and tetragonal/cubic ZrO_2, respectively) emerged by prolonging the heat-treatment process. The presence of the mentioned peaks is indicative of the $t \longrightarrow m$ phase transformation in the cooling cycles and instability of the micro-YSZ. Upon prolonging the heat-treatment duration, the weight percentage of the monoclinic phase increased from 7 to 38 wt. %. In addition, the cubic phase (62 wt. %) was also formed (50 h at 1300 °C).

According to the quantitative calculations of the XRD results based on the Rietveld method, the tetragonality values of the nano-YSZ powder were obtained as $\frac{c}{a\sqrt{2}} = \frac{5.163}{3.645\sqrt{2}} = 1.001$, $\frac{c}{a\sqrt{2}} = \frac{5.144}{3.634\sqrt{2}} = 1.0009$, $\frac{c}{a\sqrt{2}} = \frac{5.145}{3.635\sqrt{2}} = 1.0008$, and $\frac{c}{a\sqrt{2}} = \frac{5.147}{3.637\sqrt{2}} = 1.0006$ after 0, 10, 20, and 50 hours of heat-treatment, respectively, at 1300 °C (Figure 3). Qualitative and quantitative results of the XRD analysis confirmed the stability of the t´-phase ZrO_2 and absence of the cubic and monoclinic phases in the nano-YSZ samples after 50 hours of heat-treatment at 1300 °C.

In the XRD analysis of the YSZ composition, differentiation of the structures of "t" and "c" ZrO_2 requires careful examination of the (400)/(004) peaks at the angle ranges of 72-76°. The "c" phase at these angles is observed as a single peak while the "t" phase is shown in split peaks [28,29].

Figure 2 presents the peak associated with (111) and (400) plates ("m", "t", and "c") for the micro-YSZ sample after 0, 10, 20, and 50 hours of heat-treatment at 1300 °C. The peaks of (111) "m" and (400) "c" emerged by prolonging the heat-treatment duration. The presence of the mentioned peaks is indicative of the phase transformation of the "t" to the "m" during the cooling process and phase instability of the micro-YSZ compound.

$t \longrightarrow m$ phase transformation in the ZrO_2-based compounds can be thermodynamically assessed. According to the available theories mentioned in [30], the initiation temperature of $t \longrightarrow m$ phase transformation can be attributed to the stability of these two phases. The stability of these two phases depends on the surface "γ_s" and volume "γ_v" free energies of the particles. The free energy of the monoclinic phase is lower than that of the tetragonal phase ($\gamma_v^m \leq \gamma_v^t$), and the surface free energy of the tetragonal phase is lower than the monoclinic ($\gamma_s^t \leq \gamma_s^m$) one. In this situation, when the mean particle size of the ZrO_2 powder is smaller than a critical value in the given temperature ($r \leq r^*$), the role of the surface free energy (γ_s) will be more determinative than the volume free energy (γ_v) [30-33]. Therefore, the stability of the tetragonal ZrO_2 phase is thermodynamically feasible.
Upon increasing the particle size ($r \geq r^*$), the monoclinic phase will be stable. Therefore, in the case of nano-YSZ, the particle size of the ZrO_2 powder after 50 hours of heat treatment at 1300 °C is still smaller than the critical size (r^*) to provide the possibility of $t \longrightarrow m$ phase

transformation; therefore, the thermodynamic condition of transformation from the tetragonal to monoclinic phases is not fulfilled. In the case of micro-YSZ, the larger initial sizes of the ZrO_2 particles in addition to their growth during the heat-treatment process provided the thermodynamic condition for $t \longrightarrow m$ phase transformation.

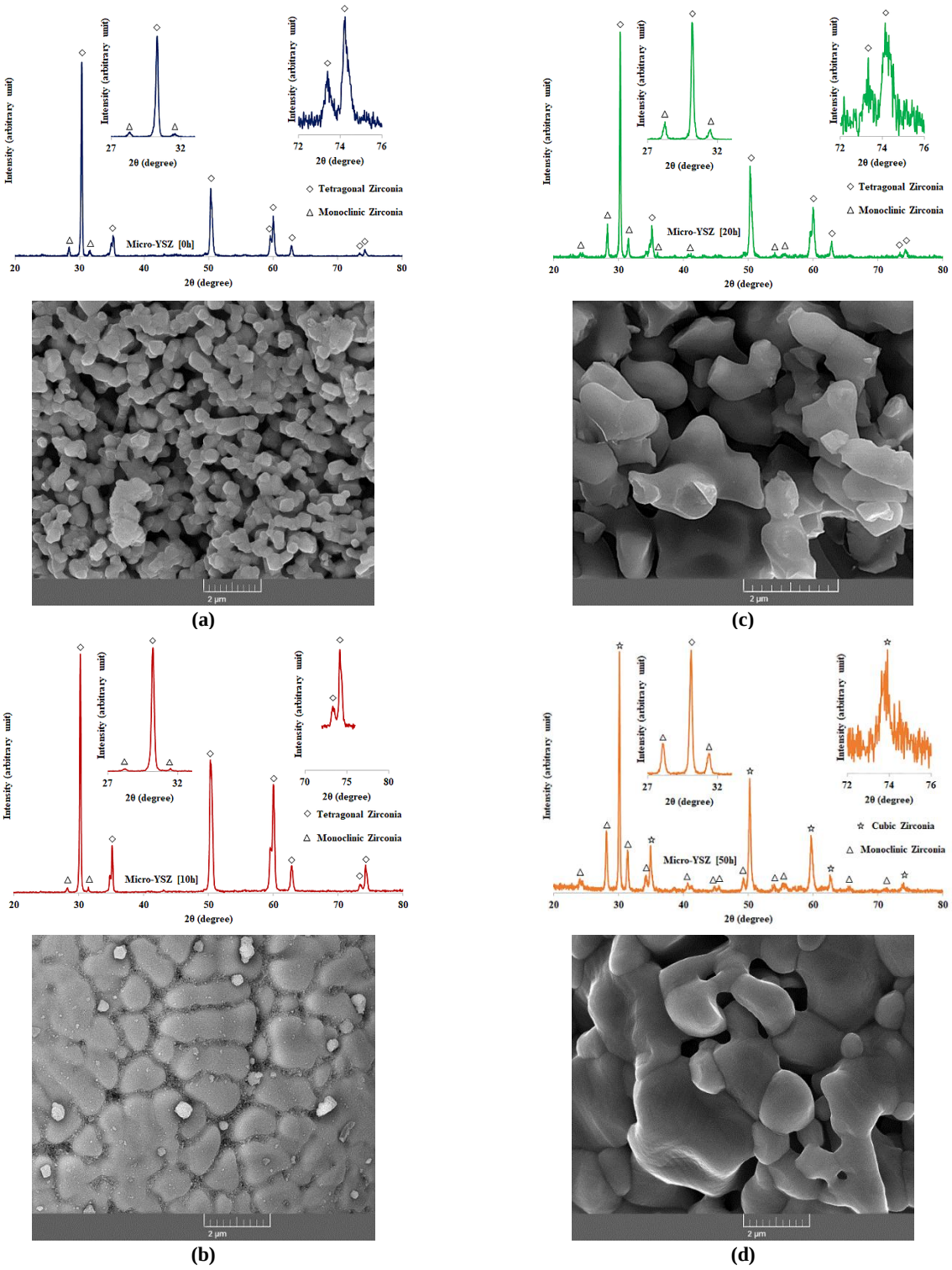

Figure 2. Results of XRD and FESEM analyses of the commercial micro-YSZ powder before and after heat treatment for (a) 0 h, (b) 10 h, (c) 20 h, and (d) 50 h at 1300 ºC

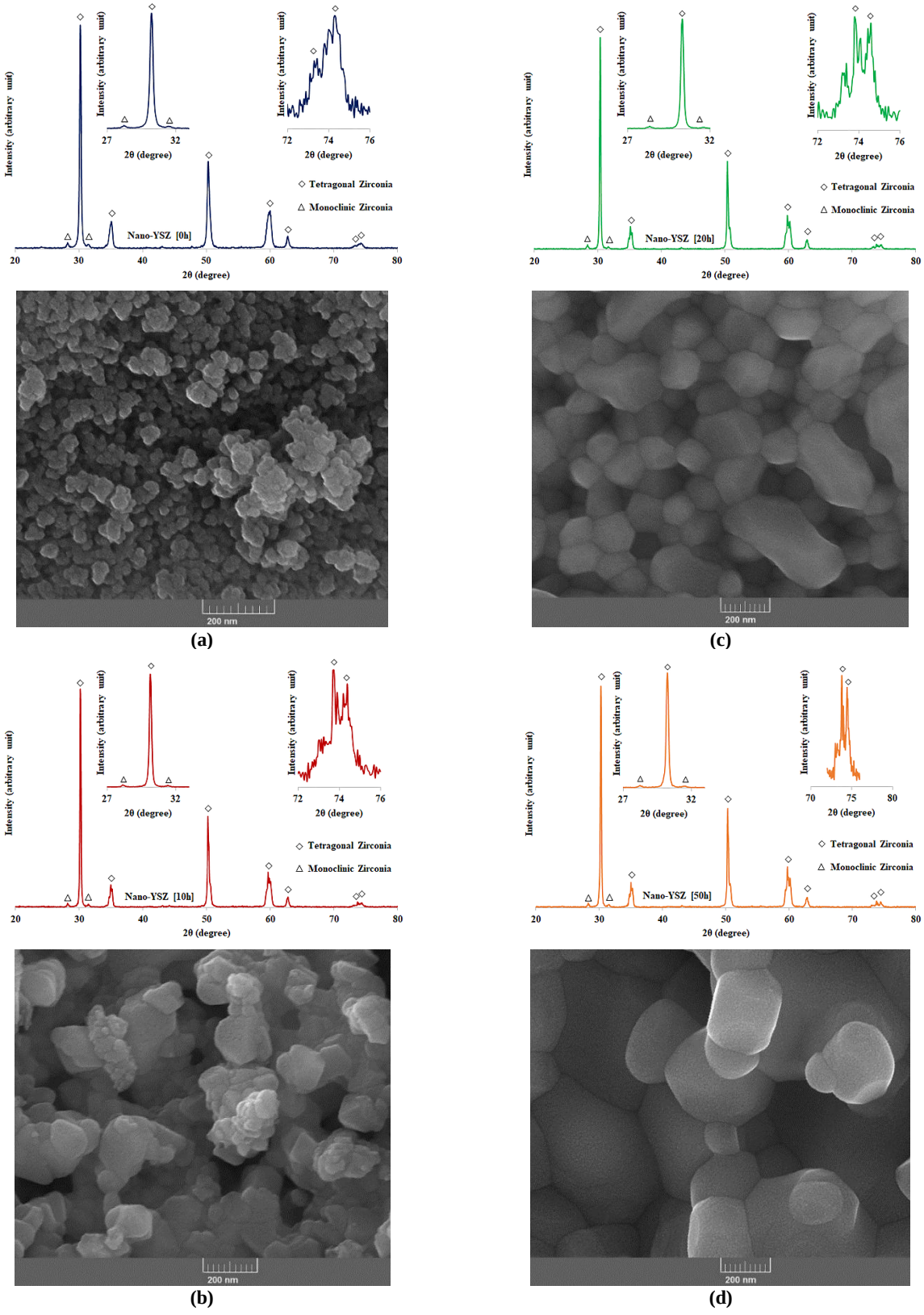

Figure 3. Results of XRD and FESEM analyses of the synthesized nano-YSZ powder before (calcinated at 1000 ºC for two hours) and after heat treatment for (a) 0 h, (b) 10 h, (c) 20 h, and (d) 50 h at 1300 ºC

For a better understanding of this phenomenon, the thermodynamic relations were also evaluated. In Equation (2), G shows the free energy of the spherical particles, r their diameter, γ the surface energy. Equation (3) was proposed to calculate the difference in the free energies of the tetragonal and monoclinic phases. Followed by computing the critical radius and differentiating Equation (3), we will have Equation (4) [31,34].

$$G = \frac{4}{3}\pi r^3 G_v + 4\pi r^2 \gamma \quad (2)$$

$$\Delta G(r) = \frac{4}{3}\pi r^3 \Delta G_v + 4\pi r^2 (\gamma_t - \gamma_m) \quad (3)$$

γ_t (tetragonal) = 0.77 Jm^{-2}

γ_m (monoclinic) = 1.13 Jm^{-2}

$$r^* = -2\frac{(\gamma_t - \gamma_m)}{\Delta H(1 - \frac{T}{T_b})} \quad (4)$$

where T_b = 1175 °C shows the transformation temperature of an infinite crystal and $\Delta H = 2.82 \times 10^8$ Jm^{-3} (all determined from calorimetry studies) represents the transformation heat per unit volume of an infinite crystal [31,34].

Based on Equations (2-4), the stability of the tetragonal or monoclinic phases of ZrO_2 at different temperatures depends on their particle sizes. Therefore, the probability of $t \longrightarrow m$ phase transformation will be incremented by increasing the temperature of the heat-treatment.

Figures 2 and 3 (a-d) depict the FESEM images of micro-YSZ and nano-YSZ after heat treatment at 1300 °C for 0, 10, 20, and 50 h. The growth of ZrO_2 particles due to the sintering and application of the thermal cycles can be observed in these images. A comparison of Figure 2 and Figure 3 confirmed the growth of particles due to heat treatment at high temperatures. It seems that followed by the heat treatment at high temperatures, grain rotation among the neighboring grains occurs, producing a coherent grain–grain interface associated with the disappearance of grain boundaries and consequently with the grain coalescence. This results in a change of grain orientation and formation of some equiaxed grains. Digimizer image analysis software was used to determine the average particle size of different powders (micro-YSZ and nano-YSZ) at different heat-treatment temperatures (Figure 4).

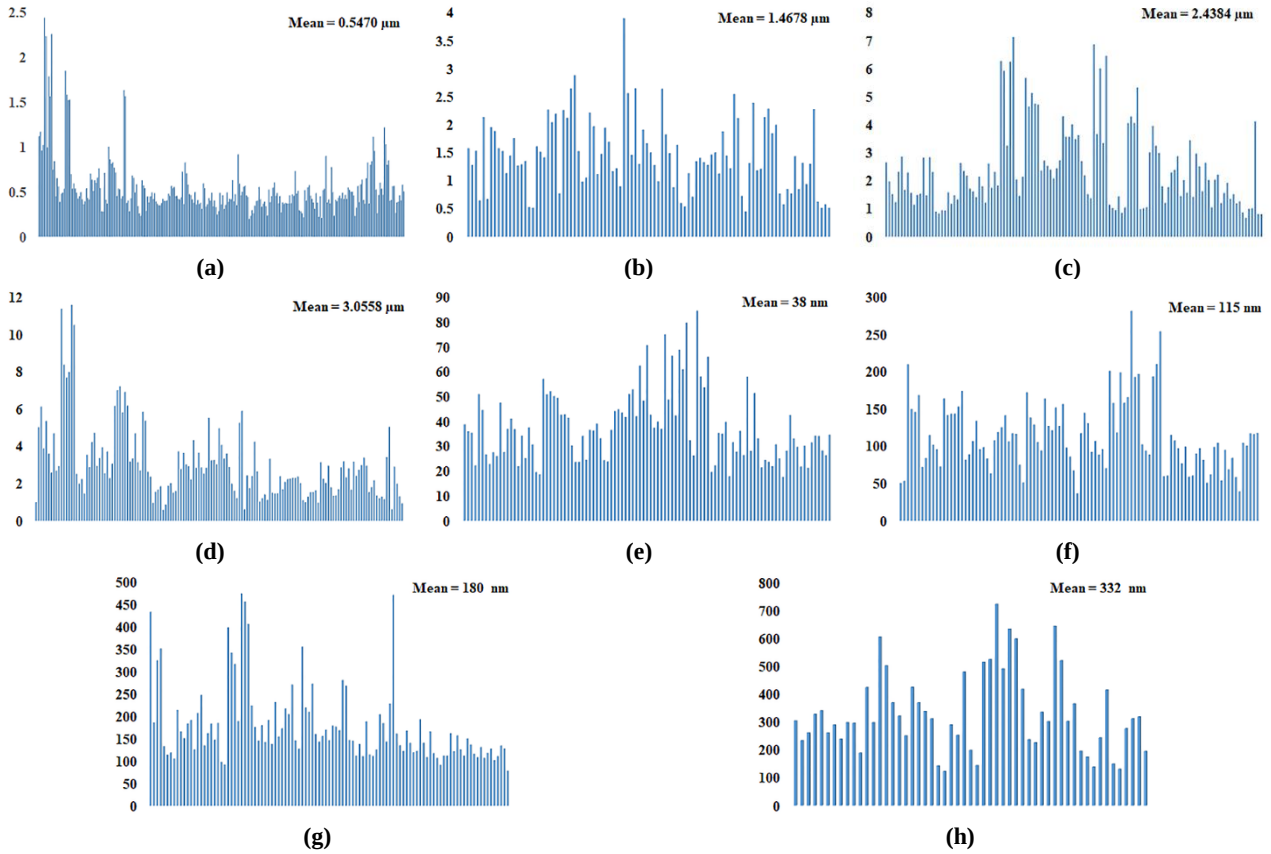

Figure 4. The average particle size of (a-d) micro-YSZ and (e-h) nano-YSZ powders at different heat-treatment temperatures

Upon extending the heat-treatment duration, the temporal variations in Full Width at Half Maximum (FWHM) parameter (Figure 5) predicts a decrease in the peak width and an increase in the particle growth rate. The FWHM variation trend in the nano-YSZ particle can be separated into two parts: in the first part (0-20 h) a steep slope is observed while in the second part (20-50 h) a linear trend is followed. It can be said that during the beginning stages of heat-treatment, the growth rate of the nano-YSZ particles was higher.

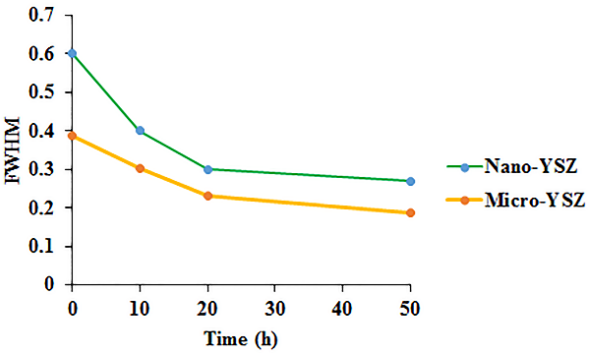

Figure 5. FWHM variation of micro- and nano-YSZ after heat-treatment at 1300 °C for 0, 10, 20, and 50 hours.

Based on the findings in this study, it can be concluded that nano-YSZ ceramic powder can be considered as a suitable candidate for potential TBC applications at ultra-high temperatures (higher than 1200 °C) owing to its improved phase stability, compares to that of micro-YSZ. However, additional research on the phase stability at longer exposure times is required to confirm this statement.

4. CONCLUSIONS

The main objective of the current study was to improve the functionality of the micro-YSZ in TBCs. Followed by synthesizing the nano-YSZ using precipitation methods and evaluating the phase stability of the samples at the working temperature of the new generation of gas turbines, the following conclusions were drawn (1300 °C):

- Based on the co-precipitation approach, nano-YSZ powder, including t'-phase, was successfully created at 1000 °C for two hours.
- The t-prime phase was not found in the heat-treated micro-YSZ after 50 hours of heat treatment at 1300 °C, indicating the instability of micro-YSZ at ultra-high temperatures.
- Investigation of the phase stability of nano-YSZ powders at 1300 °C revealed their high potential capabilities while applied to the new generation of TBCs.

ACKNOWLEDGEMENTS

The authors would like to express their gratitude to the honorable managing director of the "Barad Technology Co" (new technology-based firm, https://www.baradtechno.ir), Dr. Mahmoud Shahriari, and all of the personnel who work in the research and development department of the company.

REFERENCES

1. Rajendran, R., "Gas turbine coatings–an overview", ***Engineering Failure Analysis***, Vol. 26, (2012), 355-69. https://doi.org/10.1016/j.engfailanal.2012.07.007
2. Vaßen, R., Jarligo, M. O., Steinke, T., Mack, D. E., Stöver, D., "Overview on advanced thermal barrier coatings", ***Surface and Coatings Technology***, Vol. 205, No. 4, (2010), 938-942. https://doi.org/10.1016/j.surfcoat.2010.08.151
3. Cao, X. Q., Vassen, R., Stoever, D., "Ceramic materials for thermal barrier coatings", ***Journal of the European Ceramic Society***, Vol. 24, No. 1, (2004), 1-10. https://doi.org/10.1016/S0955-2219(03)00129-8
4. Bahamirian, M., Hadavi, S. M. M., Farvizi, M., Keyvani, A., Rahimipour, M. R., "Thermal durability of YSZ/nanostructured $Gd_2Zr_2O_7$ TBC undergoing thermal cycling", ***Oxidation of Metals***, Vol. 92, No. 5, (2019), 401-421. https://doi.org/10.1007/s11085-019-09937-7
5. Keyvani, A., Bahamirian, M., Kobayashi, A., "Effect of sintering rate on the porous microstructural, mechanical and thermomechanical properties of YSZ and CSZ TBC coatings undergoing thermal cycling", ***Journal of Alloys and Compounds***, Vol. 727, (2017), 1057-1066. https://doi.org/10.1016/j.jallcom.2017.08.184
6. Keyvani, A., Bahamirian, M., "Oxidation resistance of Al_2O_3-nanostructured/CSZ composite compared to conventional CSZ and YSZ thermal barrier coatings", ***Materials Research Express***, Vol. 3, No. 10, (2016), 105047. https://doi.org/10.1088/2053-1591/3/10/105047
7. Bahamirian, M., Hadavi, S. M. M., Farvizi, M., Rahimipour, M. R., Keyvani, A., "Enhancement of hot corrosion resistance of thermal barrier coatings by using nanostructured $Gd_2Zr_2O_7$ coating", ***Surface and Coatings Technology***, Vol. 360, (2019), 1-12. https://doi.org/10.1016/j.surfcoat.2018.12.113
8. Keyvani, A., Bahamirian, M., "Hot corrosion and mechanical properties of nanostructured Al_2O_3/CSZ composite TBCs", ***Surface Engineering***, Vol. 33, No. 6, (2017), 433-443. https://doi.org/10.1080/02670844.2016.1267423
9. Bahamirian, M., Khameneh Asl, S., "An investigation on effect of bond coat replacement on hot corrosion properties of thermal barrier coatings", ***Iranian Journal of Materials Science and Engineering***, Vol. 10, No. 3, (2013), 12-21. http://ijmse.iust.ac.ir/article-1-571-en.html
10. Padture, N. P., Gell, M., Jordan, E. H., "Thermal barrier coatings for gas-turbine engine applications", ***Science***, Vol. 296, No. 5566, (2002), 280-284. https://doi.org/10.1126/science.1068609
11. Keyvani, A., Mostafavi, N., Bahamirian, M., Sina, H., Rabiezadeh, A., "Synthesis and phase stability of zirconia-lanthania-ytterbia-yttria nanoparticles; a promising advanced TBC material", ***Journal of Asian Ceramic Societies***, Vol. 8, No. 2, (2020), 336-344. https://doi.org/10.1080/21870764.2020.1743419
12. Bahamirian, M., Hadavi, S. M. M., Farvizi, M., Rahimipour, M. R., Keyvani, A., "Phase stability of ZrO_2 $9.5Y_2O_3$ $5.6Yb_2O_3$ $5.2Gd_2O_3$ compound at 1100 °C and 1300 °C for advanced TBC

applications", ***Ceramics International***, Vol. 45, No. 6, (2019), 7344-7350. https://doi.org/10.1016/j.ceramint.2019.01.018

13. Xu, H., Wu, J., "15 - New materials, technologies and processes in thermal barrier coatings", In ***Thermal Barrier Coatings***, Woodhead Publishing, (2011), 317-328. https://doi.org/10.1533/9780857090829.3.317
14. Khor, K. A., Yang, J., "Lattice parameters, tetragonality (ca) and transformability of tetragonal zirconia phase in plasma-sprayed ZrO_2-Er_2O_3 coatings", ***Materials Letters***, Vol. 31, No. 1-2, (1997), 23-27. https://doi.org/10.1016/S0167-577X(96)00245-5
15. Pan, W., Phillpot, S. R, Wan, C., Chernatynskiy, A., Qu, Z., "Low thermal conductivity oxides", ***MRS Bulletin***, Vol. 37, No. 10, (2012), 917-922. https://doi.org/10.1557/mrs.2012.234
16. Basu, B., "Toughening of yttria-stabilised tetragonal zirconia ceramics", ***International Materials Reviews***, Vol. 50, No. 4, (2005), 239-256. https://doi.org/10.1179/174328005X41113
17. Hajizadeh-Oghaz, M., Shoja Razavi, R., Loghman-Estarki, M. R., "Synthesis and characterization of non-transformable tetragonal YSZ nanopowder by means of Pechini method for thermal barrier coatings (TBCs) applications", ***Journal of Sol-Gel Science and Technology***, Vol. 70, No. 1, (2014), 6-13. https://doi.org/10.1007/s10971-014-3266-z
18. Loghman-Estark, M. R., Razavi, R. S., Edris, H., "Synthesis and Thermal Stability of Nontransformable Tetragonal (ZrO_2) 0.96 ($REO_{1.5}$) 0.04 (Re= Sc^{3+}, Y^{3+}) Nanocrystals", In ***Defect and Diffusion Forum***, Trans Tech Publication Ltd., Vol. 334, (2013), 60-64. https://doi.org/10.4028/www.scientific.net/DDF.334-335.60
19. Zhou, F., Wang, Y., Wang, Y., Wang, L., Gou, J., Chen, W., "A promising non-transformable tetragonal YSZ nanostructured feedstocks for plasma spraying-physical vapor deposition", ***Ceramics International***, Vol. 44, No. 1, (2018), 1201-1204. https://doi.org/10.1016/j.ceramint.2017.10.012
20. Bahamirian, M., Hadavi, S. M. M., Farvizi, M., Keyvani, A., Rahimipour, M. R., "ZrO_2 9.5Y_2O_3 5.6Yb_2O_3 5.2Gd_2O_3; a promising TBC material with high resistance to hot corrosion", ***Journal of Asian Ceramic Societies***, Vol. 8, No. 3, (2020), 898-908. https://doi.org/10.1080/21870764.2020.1793474
21. Keyvani, A., Mahmoudinezhad, P., Jahangiri, A., Bahamirian, M., "Synthesis and characterization of $((La_{1-x}Gd_x)_2Zr_2O_7$; x= 0, 0.1, 0.2, 0.3, 0.4, 0.5, 1) nanoparticles for advanced TBCs", ***Journal of the Australian Ceramic Society***, Vol. 56, No. 4, (2020), 1543-1550. https://doi.org/10.1007/s41779-020-00500-1
22. Keyvani, A., Bahamirian, M., Esmaeili, B., "Sol-gel synthesis and characterization of ZrO_2-25wt.%CeO_2-2.5wt.%Y_2O_3 (CYSZ) nanoparticles", ***Ceramics International***, Vol. 46, No. 13, (2020), 21284-21291. https://doi.org/10.1016/j.ceramint.2020.05.219
23. Bahamirian, M., Hadavi, S. M. M., Rahimipour, M. R, Farvizi, M., Keyvani, A., "Synthesis and characterization of yttria-stabilized zirconia nanoparticles doped with ytterbium and gadolinium: ZrO_2 9.5 Y_2O_3 5.6 Yb_2O_3 5.2 Gd_2O_3", ***Metallurgical and Materials Transactions A***, Vol. 49, No. 6, (2018), 2523-2532. https://doi.org/10.1007/s11661-018-4555-x
24. Hajizadeh-Oghaz, M., Shoja Razavi, R., Ghasemi, A., "Synthesis and characterization of ceria–yttria co-stabilized zirconia (CYSZ) nanoparticles by sol–gel process for thermal barrier coatings (TBCs) applications", ***Journal of Sol-Gel Science and Technology***, Vol. 74, No. 3, (2015), 603-612. https://doi.org/10.1007/s10971-015-3639-y
25. Guo, L., Li, M., Ye, F., "Phase stability and thermal conductivity of RE_2O_3 (RE= La, Nd, Gd, Yb) and Yb_2O_3 co-doped Y_2O_3 stabilized ZrO_2 ceramics", ***Ceramics International***, Vol. 42, No. 6, (2016), 7360-7365. https://doi.org/10.1016/j.ceramint.2016.01.138
26. Li, Q. L., Cui, X. Z., Li, S. Q., Yang, W. H., Wang, C., Cao, Q., "Synthesis and phase stability of scandia, gadolinia, and ytterbia co-doped zirconia for thermal barrier coating application", ***Journal of Thermal Spray Technology***, Vol. 24, No. 1-2, (2015), 136-143. https://doi.org/10.1007/s11666-014-0158-2
27. Viazzi, C., Bonino, J. P., Ansart, F., Barnabé, A., "Structural study of metastable tetragonal YSZ powders produced via a sol–gel route", ***Journal of Alloys and Compounds***, Vol. 452, No. 2, (2008), 377-383. https://doi.org/10.1016/j.jallcom.2006.10.155
28. Sheu, T. S., Tien, T. Y., Chen, I. W., "Cubic-to-tetragonal (t') transformation in zirconia-containing systems", ***Journal of the American Ceramic Society***, Vol. 75, No. 5, (1992), 1108-1116. https://doi.org/10.1111/j.1151-2916.1992.tb05546.x
29. Srinivasan, R., De Angelis, R. J., Ice, G., Davis, B. H., "Identification of tetragonal and cubic structures of zirconia using synchrotron x-radiation source", ***Journal of Materials Research***, Vol. 6, No. 6, (1991), 1287-1292. https://doi.org/10.1557/JMR.1991.1287
30. Suresh, A., Mayo, M. J., Porter, W. D., Rawn, C. J., "Crystallite and grain-size-dependent phase transformations in yttria-doped zirconia", ***Journal of the American Ceramic Society***, Vol. 86, No. 2, (2003), 360-362. https://doi.org/10.1111/j.1151-2916.2003.tb00025.x
31. Chraska, T., King, A. H., Berndt, C. C., "On the size-dependent phase transformation in nanoparticulate zirconia", ***Materials Science and Engineering: A***, Vol. 286, No. 1, (2000), 169-178. https://doi.org/10.1016/S0921-5093(00)00625-0
32. Garvie, R. C., Goss, M. F., "Intrinsic size dependence of the phase transformation temperature in zirconia microcrystals", ***Journal of Materials Science***, Vol. 21, No. 4, (1986), 1253-1257. https://doi.org/10.1007/BF00553259
33. Garvie, R. C., "The occurrence of metastable tetragonal zirconia as a crystallite size effect", ***The Journal of Physical Chemistry***, Vol. 69, No. 4, (1965), 1238-1243. https://doi.org/10.1021/j100888a024
34. Shukla, S., Seal, S., "Mechanisms of room temperature metastable tetragonal phase stabilisation in zirconia", ***International Materials Reviews***, Vol. 50, No. 1, (2005), 45-64. https://doi.org/10.1179/174328005X14267